Density Functional Study of the [2+2]- and [2+3]-Cycloaddition Mechanisms for the Osmium-Catalyzed Dihydroxylation of Olefins

Maricel Torrent,[†] Liqun Deng,[‡] Miquel Duran,[†] Miquel Sola,[†] and Tom Ziegler*[,‡]

Departments of Chemistry, University of Girona, Girona, Spain, and University of Calgary, Calgary, Alberta T2N 1N4, Canada

Received September 12, 1996[⊗]

The postulated intermediates in the base-free and base-assisted addition of OsO_4 to olefins have been optimized using density functional theory (DFT). Ammonia was chosen as the base and ethylene as the olefin. The corresponding transition states have been characterized fully. Further, the activation barriers have been computed at the nonlocal level, and special attention has been given to the two different mechanistic hypothesis proposed for this reaction. In particular, the hypothesis by Sharpless of a [2+2]-cycloaddition pathway involving the formation of a four-member ring as an intermediate has been ruled out since the corresponding activation barrier was calculated to be as high as 39 kcal mol^{-1}. The addition of a NH_3 ligand to the osmium catalyst does not reduce significantly the [2+2] energy barrier. By contrast, it seems perfectly feasible that the dihydroxylation reaction proceeds through a [2+3] mechanism leading to the formation of a five-member ring intermediate as claimed by Corey. Such a process is found to be clearly exothermic and to involve a very small activation barrier of less than 2 kcal mol^{-1}. A detailed analysis of the sequence describing exactly how the cycloaddition proceeds along the reaction path has also been performed by means of intrinsic reaction coordinate (IRC) calculations for the two studied mechanisms.

Introduction

Certain oxo−metal compounds play a key role in organic synthesis because of their ability to selectively attach oxygen atoms to olefinic bonds. Among the high oxidation state transition metal oxides, osmium tetraoxide is one of the most effective reagents for cis-dihydroxylation of alkenes to give the corresponding vicinal diols,[1,2] Scheme 1.

It has long been recognized[3] that the rate of reaction of OsO_4 with olefins is greatly increased in the presence of tertiary amines. Thus, OsO_4 reacts with monodentate tertiary amines under nonreducing conditions to give the adducts $LOsO_4$ (L = pyridine,[3,4] isoquinoline,[5] phthalazine,[5] ammonia,[6] or dihydroquinidine derivatives[7,8]).

The key to the high selectivity and great scope found in osmium tetraoxide's reaction with olefin resides of course in the mechanism and specifically in the sequence by which the two oxygen atoms are transferred from osmium to olefin. Several mechanistic proposals have been advanced for the dihydroxylation process. Iniatially,[9] the mechanism was thought to proceed via a *concerted* [2+3] cycloaddition of two oxygen atoms to the olefin bond, Scheme 2.

Scheme 1

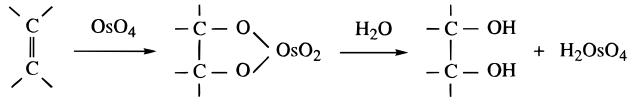

Scheme 2

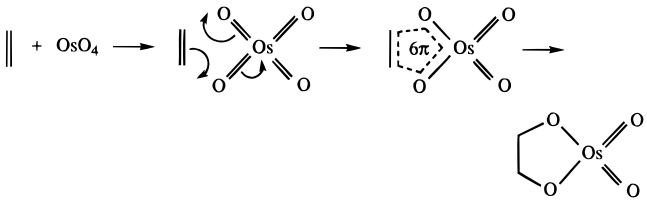

Later, Sharpless[10−14] et al. suggested a stepwise mechanism involving a [2+2]-like addition of the olefin

[†] University of Girona.
[‡] University of Calgary
[⊗] Abstract published in *Advance ACS Abstracts,* December 15, 1996.

(1) (a) Carey, F. A.; Sundberg, R. J. *Advanced Organic Chemistry, Part B: Reactions and Synthesis*; Plenum Press: New York, 1977. (b) Nugent, W. A.; Mayer, J. M. *Metal-Ligand Multiple Bonds*; Wiley: New York, 1988.
(2) Schroder, M. *Chem. Rev.* **1980**, *80*, 187.
(3) Criegee, R.; Marahand, B.; Wannowius, H. *Justus Liebigs Ann. Chem.* **1942**, *550*, 99.
(4) (a) D'yachenko, Yu. I. *Sovrem. Probl. Khim.* **1973**, 17. (b) D'yachenko, Yu. I. *Chem. Abstr.* **1974**, *81*, 130291d.
(5) (a) Cleare, M. J.; Hydes, P. C.; Griffith, W. P.; Wright, M. J. *J. Chem. Soc., DaltonTrans.* **1977**, 941. (b) Wright, M. J. Ph.D. Thesis, University of London, 1977.
(6) (a) Hair, M. L.; Robinson, P. L. *J. Chem. Soc.* **1958**, 106. (b) Hair, M. L.; Robinson, P. L. *J. Chem. Soc.* **1960**, 2775.
(7) Norrby, P. O.; Becker, H.; Sharpless, K. B. *J. Am. Chem. Soc.* **1996**, *118*, 35.
(8) Corey, E. J.; Noe, M. C. *J. Am. Chem. Soc.* **1996**, *118*, 319.
(9) (a) Dewar, M. J. S. *Ind. Chim. Belg.* **1950**, *15*, 181; *Chem. Zentralbl.* **1951**, *1*, 1716. (b) Dewar, M. J. S.; Longuet-Higgins, H. C. *Proc. R. Soc. London, Ser. A* **1952**, *214*, 482. (c) Dewar, M. J. S. *J. Am. Chem. Soc.* **1952**, *74*, 3341.
(10) Sharpless, K. B.; Teranishi, A. Y.; Backvall, J.-E. *J. Am. Chem. Soc.* **1977**, *99*, 3120.
(11) (a) Patrick, D. W.; Truesdale, L. K.; Biller, S. A.; Sharpless, K. B. *J. Org. Chem.* **1978**, *43*, 2628. (b) Hentges, S. G.; Sharpless, K. B. *J. Am. Chen. Soc.* **1980**, *102*, 4263.
(12) (a) Pearlstein, R. M.; Blackburn, B. K.; Davis, W. M.; Sharpless, K. B. *Angew. Chem., Int. Ed. Engl.* **1990**, *29*, 639. (b) Gobel, T.; Sharpless, K. B. *Angew. Chem., Int. Ed. Engl.* **1993**, *32*, 1329.
(13) (a) Norrby, P.-O.; Kolb, H. C.; Sharpless, K. B. *J. Am. Chem. Soc.* **1994**, *116*, 8470. (b) Becker, H.; Ho, P. T.; Kolb, H. C.; Loren, S.; Norrby, P.-O.; Sharpless, K. B. *Tetrahedron Lett.* **1994**, *35*, 7315.

S0276-7333(96)00783-2 CCC: $14.00

Scheme 3

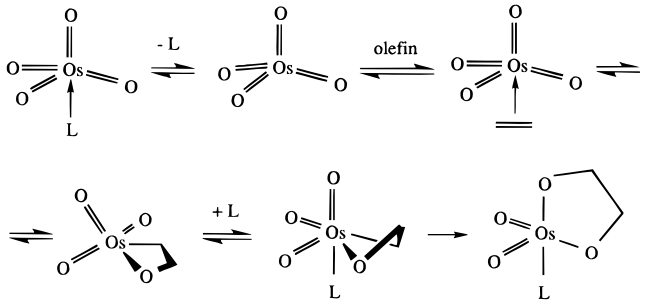

Scheme 4

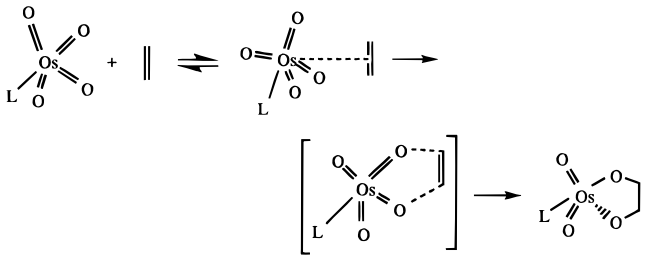

to an Os−O bond, leading to a four-membered osmaoxetane intermediate. This intermediate is then considered to rearrange in a subsequent rate-determining step to a five-membered cyclic ester complex, Scheme 3. According to a recent work by Sharpless,[7] experimental facts based on the relationship between temperature and enantioselectivity do not support a concerted [2+3] mechanism.

Corey and Noe,[8] by contrast, have argued against the [2+2]-cycloaddition pathway claimed by Sharpless. These authors have recently reported kinetic, structural and stereochemical data which strongly support a different mechanism involving: (a) rapid, reversible formation of an olefin−Os(VIII) π−d complex and (b) slow rearrangement to a [2+3]-cycloaddition transition state, Scheme 4. Additional evidence against a metallaoxetane-like transition state has also been obtained from a $^{12}C/^{13}C$ kinetic isotop effects study.[15]

From the theoretical point of view,[14,16−19] several studies have dealt with the cis-dihydroxylation of alkenes by OsO_4. Perhaps the most extensive investigation is that of Veldkamp and Frenking,[18] who thoroughly analyzed the thermochemistry corresponding to the osmylation reaction in the presence of bases, using quantum mechanical *ab initio* methods. These authors, however, were not able to report any transition state structure for the processes under study, and consequently, they did not manage to rule out any of the suggested mechanisms. A similar work was performed by Norrby[14] et al., who calculated the structure of several ruthenium complexes using DFT. Again, Norrby[14] et al. did not provide any transition state structures.

Our goal in the present study is then to provide a critical analysis of the [2+2] and [2+3] mechanisms on the basis of calculated transition state structures, activation barriers, and reaction paths. The present calculations are based on approximate density functional theory,[20] which over the past decade has been employed successfully to solve many problems previously covered exclusively by *ab initio* Hartree−Fock (HF), and post-HF methods. The recently acquired popularity of approximate DFT stems in large measure from its computational expedience which makes it amenable even to large-size molecules at a fraction of the time required for post-HF calculations. This is in particular the case for systems involving transition metals.[21] The ability of DFT to predict transition state structures and activation energies has been studied for both transition metal complexes[22a,b] and main group compounds.[22c−h]

Computational Methods

The reported calculations were carried out by using the Amsterdam density functional (ADF) package developed by Baerends[23] et al. and vectorized by Ravenek.[24] The numerical integration procedure applied for the calculations is that of te Velde and Baerends.[25] An uncontracted triple-ζ STO basis set was used for describing the 5s, 5p, 5d, 6s, and 6p orbitals of osmium. For carbon (2s, 2p), oxygen (2s, 2p), nitrogen (2s, 2p), and hydrogen (1s), double-ζ basis sets were employed and augmented by an extra polarization function.[26,27] Electrons in lower shells were treated within the frozen core approximation.[23] A set of auxiliary s, p, d, f, and g functions, centered in all nuclei, was introduced in order to fit the molecular density and Coulomb potential accurately in each SCF cycle.[28] All the geometries and frequencies were calculated at the local density approximation (LDA) level[29] with the parametrization of Vosko[30] et al. The relative energies were evaluated by including Becke's nonlocal exchange[31] and Perdew's nonlocal correlation corrections[32] as perturbations based on the LDA density. This approach is denoted NL-P, and its validity has been discussed elsewhere.[33] The geometry optimization procedure was based on an analytical gradient scheme developed

(14) Norrby, P.-O.; Kolb, H. C.; Sharpless, K. B. *Organometallics* **1994**, *13*, 344.
(15) Corey, E. J.; Noe, M. C.; Grogan, M. J. *Tetrahedron Lett.* **1996**, *37*, 4899.
(16) Rappé, A. K.; Goddard, W. A., III, *J. Am. Chem. Soc.* **1982**, *104*, 448.
(17) Jørgensen, K. A.; Hoffmann, R. *J. Am. Chem. Soc.* **1986**, *108*, 1867.
(18) Veldkamp, A.; Frenking, G. *J. Am. Chem. Soc.* **1994**, *116*, 4937.
(19) Jørgensen, K. A.; Schiott, B. *Chem. Rev.* **1990**, *90*, 1483.
(20) (a) Parr, R. G.; Yang, W. *Density-Functional Theory of Atoms and Molecules*; Oxford University Press: New York, 1989. (b) Laird, B. B, Ross, R. B., Ziegler, T., Eds. *Chemical Applications of Density Functional Theory*; ACS Symposium Series 629; American Chemical Society: Washington, DC, 1996. (c) Ziegler, T. *Chem. Rev.* **1991**, *15*, 741.
(21) (a) Ziegler, T. *Can. J. Chem.* **1995**, *73*, 743. (b) Torrent, M.; Gili, P.; Duran, M.; Sola, M. *J. Chem. Phys.* **1996**, *104*, 9499.
(22) (a) Margl, P.; Ziegler, T. *J. Am. Chem. Soc.*, in press. (b) Margl, P.; Ziegler, T. *Organometallics*, in press. (c) Deng, L.; Ziegler, T. *Int. J. Quant. Chem.* **1994**, *52*, 731. (d) Deng, L.; Ziegler, T. *J. Chem. Phys.* **1993**, *99*, 3823. (e) Deng, L.; Ziegler, T *J. Phys. Chem.* **1995**, *99*, 612. (f) Fan, L.; Ziegler, T. *J. Am. Chem. Soc.* **1992**, *114*, 10890. (g) Fan, L.; Ziegler, T. *J. Chem. Phys.* **1990**, *92*, 46. (h) Torrent, M.; Duran, M.; Sola, M. *J. Mol. Struct. (Theochem)*, in press.
(23) Baerends, E. J.; Ellis, D. E.; Ros, P. *Chem. Phys.* **1973**, *2*, 41.
(24) Ravenek, W. In *Algorithms and Applications on Vector and Parallel Computers*; te Riele, H. J. J., Dekker, T. J., van de Vorst, H. A., Eds.; Elsevier: Amsterdam, 1987.
(25) (a) Boerrigter, P. M.; te Velde, G.; Baerends, E. J. *Int. J. Quantum Chem.* **1987**, *33*, 87. (b) te Velde, G.; Baerends, E. J. *J. Comput. Phys.* **1992**, *99*, 84.
(26) (a) Snijders, G. J.; Baerends, E. J.; Vernooijs, P. *At. Nucl. Data Tables* **1982**, *26*, 483.
(27) Vernooijs, P.; Snijders, G. J.; Baerends, E. J. *Slater Type Basis Functions for the Whole Periodic System*; Internal Report; Free University of Amsterdam: Amsterdam, 1981.
(28) Krijn, J.; Baerends, E. J. *Fit Functions in the HFS-methods*; Internal Report; Free University of Amsterdam: Amsterdam, 1984.
(29) Gunnarson, O.; Lundquist, I. *Phys. Rev.* **1974**, *10*, 1319.
(30) Vosko, S. H.; Wilk, L.; Nusair, M. *Can. J. Phys.* **1980**, *58*, 1200.
(31) Becke, A. D. *Phys. Rev. A* **1988**, *38*, 2398.
(32) (a) Perdew, J. P. *Phys. Rev. Lett.* **1985**, *55*, 1655. (b) Perdew, J. P. *Phys. Rev. B* **1986**, *33*, 8822. (c) Perdew, J. P.; Wang, Y. *Phys. Rev. B* **1986**, *33*, 8800.
(33) (a) Deng, L.; Ziegler, T. *Organometallics* **1996**, *15*, 3011. (b) Ziegler, T.; Li, J. *Organometallics* **1995**, *14*, 214. (c) Deng, L.; Ziegler, T. *Organometallics*, submitted for publication.

by Versluis[34] and Ziegler. The harmonic vibrational frequencies were computed from the force constants obtained by numerical differentiation of the energy gradients.[35] Relativistic corrections to the total energy were taken into account by the quasirelativistic method[36a,b] (QR). The application of this scheme, in comparison to other relativistic methods, has been discussed by Li[36c] et al. Transition state structures were optimized according to the scheme by Banerjee[37a] et al. and Baker[37b] in the ADF implementation due to Fan[22g] et al. All first-order saddle points were shown to have a Hessian matrix with a single negative eigenvalue. The intrinsic reaction coordinate (IRC) method by Fukui[37c] was based on the reaction coordinate search scheme by Gonzalez and Schlegel[37d] in the ADF implementation due to Deng[22c] et al. The application of DFT to organometallic chemistry has been recently reviewed.[21a]

Results and Discussion

In the first part of this section, we present results from our calculations on the [2+2] and [2+3] addition of olefin to OsO_4 without the presence of a base. The influence of the base upon the reaction pathway is investigated in the second part. Ammonia and ethylene were chosen as model compounds for the base and olefin, respectively.

Base-Free [2+2] Addition of Ethylene to Osmium Tetraoxide. Figure 1 displays the optimized geometries for the stationary points on the reaction path corresponding to the [2+2]-cycloaddition potential energy surface. All structures were optimized without symmetry constraints.

Structure **1a** corresponds to the tetrahedrally symmetric osmium catalyst. The TS structure, **1b**, has a single imaginary frequency of 764i cm^{-1}, with the next three lower frequencies at 61, 115, and 228 cm^{-1}, respectively. The normal mode corresponding to the imaginary frequency represents a displacement along the emerging C−O bond. The ring closure finishes up in the metallacycle, **1c**, which is the product for the [2+2] cycloaddition. In **1c**, the C−O distance has decreased to a typical bond length for a C−O single bond (1.43 Å), and the two carbon centers have undergone an sp^2 to sp^3 rehybridization.

The energy profile for the base-free [2+2] cycloaddition, Figure 2, reveals that the reaction is endothermic. The osmaoxetane, **1c**, lies about 3.7 kcal mol^{-1} above the two reacting species, **1a** + C_2H_4. It can also be seen from the asymmetric profile that **1b** is a productlike TS. Even more significant is the fact that the reaction has a large activation barrier of 39.7 kcal mol^{-1}. The formation of the osmaoxetane intermediate, **1c**, is, therefore, unlikely to take place under the experimentally mild conditions usually employed in the osmium-catalyzed dihydroxylation of olefins.[8] At room temperature such a barrier is unsurmountable.

A further detailed description of the reaction is given in Figure 3. Here, we display changes in key internal coordinates along the IRC. The IRC was constructed

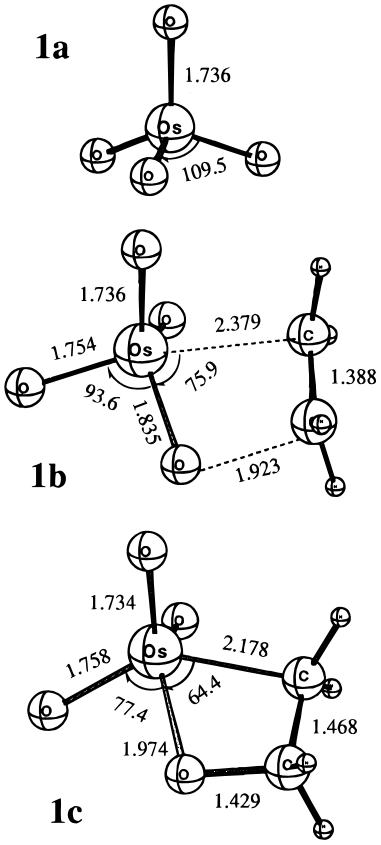

Figure 1. Optimized geometries for the stationary points along the base-free [2+2]-cycloaddition reaction path: Reactant, **1a**; transition state, **1b**; the osmaoxetane product, **1c**. Bond lengths are in Å, and bond angles are in degrees.

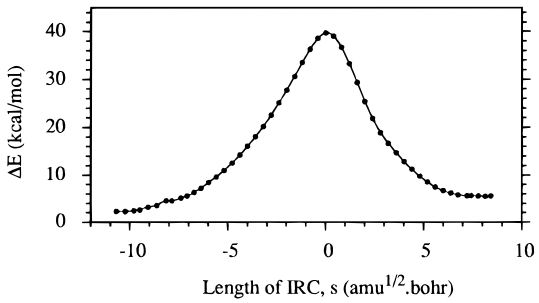

Figure 2. Energy profile for the [2+2]-cycloaddition reaction along the IRC path. The length of the IRC is given by s (amu$^{1/2}$ bohr). Definitions: ΔE, energies relative to free OsO_4 and C_2H_4; $s = 0.0$, the transition state; $s \approx 8.5$, the cycloaddition product; $s \rightarrow -\infty$, $OsO_4 + C_2H_4$.

from a total of 100 steps. Starting from the reactants, **1a** + C_2H_4, the ethylene molecule is gradually brought together with the osmium complex until reaching the product, **1c** ($s = 8.5$). The most remarkable changes taking place in the path from **1a** + C_2H_4 to the TS, **1b** ($s = 0.0$) are the shortening of the R(Os−C) and R(C−O) distances almost linearly with s. Notice that in the early stages of the reaction when the interaction between the two reactants is still very weak, the O−Os−O bond angles (*ad*/*ac*/*ab*) tend to become smaller in order to better assist the approach of the olefin. The variation in the dihedral angle *bfg* indicates that the four-membered ring becomes more coplanar as the olefin approaches OsO_4, from an initial tilt angle of 13° until a minimum (around $s \approx 3.0$) where it has decreased to 5°. In this region prior to TS, the other internal coordinates remain nearly unaffected.

(34) (a) Versluis, L.; Ziegler, T. *J. Chem. Phys.* **1988**, *88*, 322. (b) Fan, L.; Ziegler, T. *J. Chem. Phys.* **1991**, *95*, 7401. (c) Schreckenback, G.; Li, J.; Ziegler, T. *Int. J. Quantum Chem.* **1995**, *56*, 477.

(35) (a) Fan, L.; Versluis, L.; Ziegler, T.; Baerends, E. J.; Ravenek, W. *Int. J. Quantum Chem. Symp.* **1988**, *22*, 173.

(36) (a) Ziegler, T.; Tschinke, V.; Baerends, E. J.; Snijders, J. G.; Ravenek, W. *J. Phys. Chem.* **1989**, *93*, 3050. (b) Schreckenbach, G.; Ziegler, T.; Li, J. *Int. J. Quantum Chem.* **1995**, *56*, 477.

(37) (a) Banerjee, A.; Adams, N.; Simons, J.; Shepard, R. *J. Phys. Chem.* **1985**, *89*, 52. (b) Baker, J. *J. Comput. Chem.* **1986**, *7*, 385. (c) Fukui, K. *Acc. Chem. Res.* **1981**, *14*, 363. (d) Gonzalez, C.; Schlegel, H. B. *J. Phys. Chem.* **1990**, *94*, 5523.

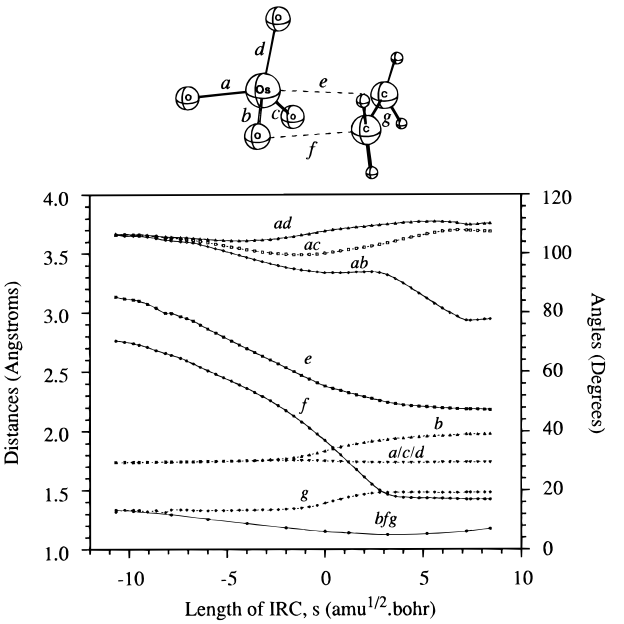

Figure 3. Change of internal coordinates for the [2+2]-cycloaddition reaction along the IRC path. The length of the IRC is given by s (amu$^{1/2}$ bohr). Definitions: $s = 0.0$, the transition state, **1b**; $s \approx 8.5$, the product, **1c**; $s \rightarrow -\infty$, the reactants, **1a** + C_2H_4.

It is worthwhile to notice that one of the crucial chemical changes of this reaction, which is the conversion from an olefinic bond to a C−C single bond, occurs *around* as well as immediately *after* the TS in the case of the [2+2] mechanism. Thus, as displayed by *g* in Figure 3, it is not until $s \approx 0.0$ that the olefin starts losing its double-bond character. Notice that, as soon as the *R*(C−C) bond length becomes stable (at $s \approx 3.0$), the *R*(C−O) distance also becomes constant (1.43 Å). At this point in the path ($s = 3.0$) the four atoms involved in the ring practically occupy the same positions as in the final intermediate, **1c**. However, the energy still decreases due to the favorable change occuring in the *ab* angle. This bond angle experiences a steady decrease starting precisely at $s \approx 3.0$ (94°) and finishing close to the product around $s = 7.2$ (78°).

Aside from the stretching of the olefinic C−C bond, the other main process responsible for the large activation barrier seems to be the Os−O bond stretch. As can be seen from Figure 3, the *R*(Os−O) bond distance depicted by *b* begins to stretch at $s = -3.1$ (1.74 Å), and once the TS has been reached, it continues increasing smoothly until **1c** (1.97 Å). The remaining three Os−O bonds (*a*/*c*/*d*) are nearly constant along the reaction path.

Let us turn now our attention to the sequence of the reaction. There has been some debate as to whether the [2+2] cycloaddition would proceed initially as an electrophilic or nucleophilic attack of OsO_4 on olefin. Veldkamp and Frenking[18] investigated the orbital energies of the frontier orbitals in OsO_4, and in light of their results, they suggested that the [2+2] reaction should be considered as an initial nucleophilic attack of the osmium complex on olefin. More specifically, they predicted that first one oxygen atom attacks nucleophilically an olefinic carbon, and then, the other carbon attacks electrophilically the osmium atom, yielding the postulated four-member intermediate. However, it has been shown[38] that electron-withdrawing groups on the olefin retard its reactivity toward OsO_4, which is

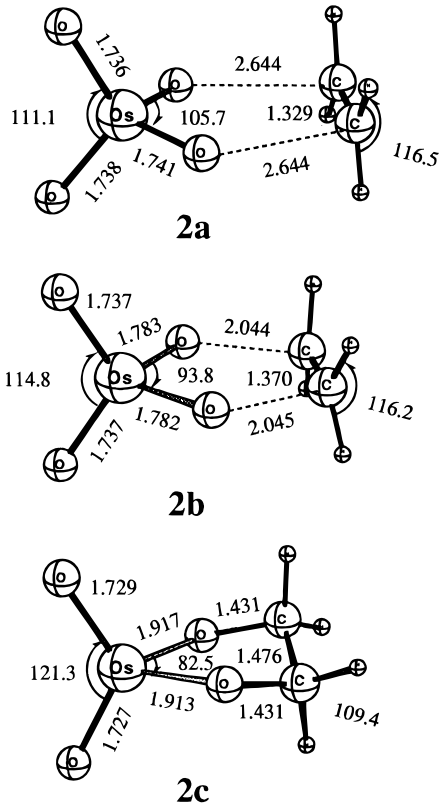

Figure 4. Optimized geometries for the stationary points along the base-free [2+3]-cycloaddition reaction path: Adduct, **2a**; transition state, **2b**; five-membered ring product, **2c**. Bond lengths are in Å, and bond angles are in degrees.

evidence against the rate-determining nucleophilic reaction step proposed by Veldkamp and Frenking,[18] at least if the [2+2] addition is involved in osmium-catalyzed dihydroxylation of olefins.

Our calculations suggest, on the other hand, an initial nucleophilic attack of the olefinic carbon on the metal center *before* and around the TS, followed by a nucleophilic attack of an oxygen atom on the other olefinic carbon *after* the TS has been reached, Figure 3. In effect, from the initial stages of the process up to the TS, **1b**, both the *R*(Os−C) and the *R*(C−O) distances have been decreased by roughly the same amount, as shown by the parallel lines for *e* and *f* in the region $-10.8 < s < -1.0$, Figure 3. By contrast, on the product side of the pathway up to the final metallacycle, **1c**, the *R*(Os−C) distance shortens only 0.2 Å whereas the length of the C−O bond decreases by more than 0.5 Å. In particular, the main difference between *e* and *f* (Figure 3) occurs in the region $0.0 < s < 3.0$, where the curvature for *e* tends to flatten, whereas the slope for *f* becomes more negative. It is thus clear from the changes in the *R*(Os−C) and *R*(C−O) distances along the IRC, Figure 3, that Os−C bond making is ahead of C−O bond formation in the [2+2] cycloaddition. Folga[39] et al. have recently reported an analogous conclusion for the formation of a four-center metallacycle from ethylene and molybdenum carbene.

Base-Free [2+3] Addition of Ethylene to Osmium Tetraoxide. Figure 4 displays the optimized

(38) (a) Badger, G. M. *J. Chem. Soc.* **1949**, 456. (b) Henbest, H. B.; Jackson, W. R.; Robb, B. C. G. *J. Chem. Soc. B* **1966**, 803. (c) Sharpless, K. B.; Williams, D. R. *Tetrahedron Lett.* **1975**, 3045. (d) Marko, I. E. *Proceedings of the Chiral Synthesis Symposium and Workshop*; Spring Innovations Ltd.: Stockport, England, 1989; pp 13−21.

(39) Folga, E.; Ziegler, T. *Organometallics* **1993**, *12*, 325.

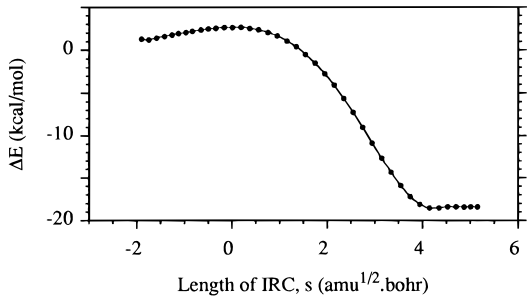

Figure 5. Energy profile for the [2+3]-cycloaddition reaction along the IRC path. The length of the IRC is given by *s* (amu$^{1/2}$ bohr). Definitions: ΔE, energies relative to free OsO_4 and C_2H_4, $s = 0.0$, the transition state; $s \approx 4.5$, the cycloaddition product; $s \rightarrow -\infty$, $OsO_4 + C_2H_4$.

molecular structures for the species involved in a [2+3]-cycloaddition reaction. In the early stages of the process, a symmetrical adduct, **2a**, is formed. At this point, the interaction between C_2H_4 and OsO_4 is expected to be very weak since **2a** is only 0.2 kcal mol^{-1} more stable than the separated reactant species. The bond angle between the two oxygen atoms pointing toward the C=C double bond in **2a** is only 3.8° smaller than in the free reactant **1a** (109.5°). The transition state, **2b**, does not differ remarkably from the adduct. In comparison to **2a**, the transition state, **2b**, exhibits further shortening of the C−O distances and closing of the O−Os−O bond angle in the emerging five-membered ring. At the same time an opening takes place of the O−Os−O bond angle in the plane perpendicular to the ring. Further, in the TS the two carbon centers still retain their initial sp^2 hybridization, and the whole structure can still be considered to have a C_{2v} symmetry. As in **2a**, the five atoms of the incipient ring in **2b** are still coplanar. Thus, **2b** can be considered a reactant-like TS. This is in good agreement to the energy profile displayed in Figure 5. The reactant side of this process has a very flat energy profile, as confirmed by the four lower frequencies of the TS **2b** (−85, 96, 118, and 195 cm^{-1}). If we come back to Figure 4, the reaction finally leads to the five-membered ring labeled as **2c**. In this species, not only do the carbon atoms display sp^3 hybridization but also the O−C−C−O fragment exhibits the typical shape and distances of a diol skeleton.

As far as energy considerations are concerned, Figure 5 reveals that the path for the [2+3] cycloaddition is clearly exothermic, since the five-membered intermediate **2c** is 20.6 kcal mol^{-1} more stable than the two reacting species. A similar qualitative conclusion was also found by Veldkamp[18] and Frenking. In their study, the osmium ester complex was reported to be 12.2 kcal mol^{-1} lower in energy than the reactants. However, if we come back to Figure 5, more important is the fact that only a very small activation barrier of 1.8 kcal mol^{-1} must be surmounted in order for the reaction to proceed through a [2+3]-addition mechanism. Unlike the [2+2] mechanism discussed in the previous section (Figure 2), the [2+3] pathway seems to be perfectly feasible.

Figure 6 contains all information concerning the way in which the [2+3] reaction proceeds. It represents the change in the internal coordinates as a function of the IRC length *s*, from −2.0 to 4.5. The IRC was constructed from a total of 80 steps. The natural reaction coordinate for the [2+3] cycloaddition is the *R*(C−O) distance (*e* or *f*) which varies linearly with *s* from 2.28

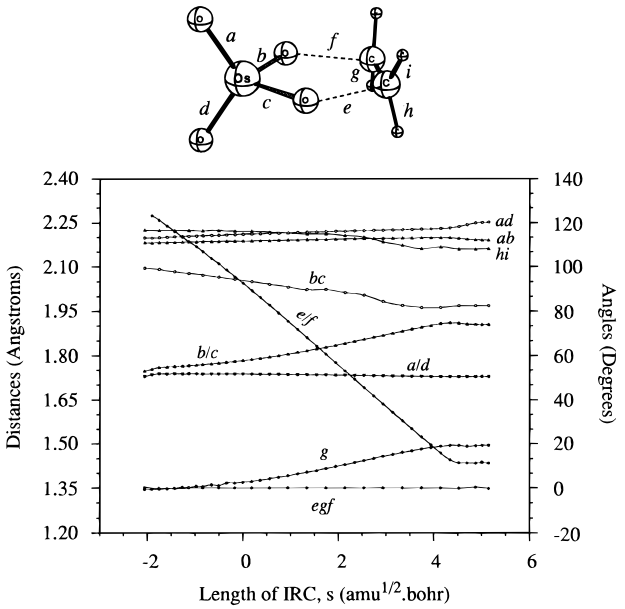

Figure 6. Change of internal coordinates for the [2+3]-cycloaddition reaction along the IRC path. The length of the IRC is given by *s* (amu$^{1/2}$ bohr). Definitions: $s = 0.0$, the transition state, **2b**; $s \approx 8.5$, the product, **2c**; $s \rightarrow -\infty$, the reactants, $OsO_4 + C_2H_4$.

Å at $s = -2.0$ to 1.48 Å in the region close to **2c**. Another highlighted change is the closing of the *bc* bond angle (which could alternatively describe the reaction). However, this change is not as linear as in the case of *R*(C−O) distance, especially in the second half of the reaction path. As also expected from Figures 2 and 5, not many structural changes occur in the path from the reactants to **2b** ($s = 0.0$). By contrast, significant structural changes occur on the product side of the reaction leading to the ester complex **2c**. Thus, the stretching of the two Os−O bonds (*b*/*c*) becomes more pronounced once the TS has been reached ($s > 0.0$). Even clearer is the case of the C−C bond elongation (*g*), where the conversion from an olefinic to a single bond can be considered to take place *after* the TS. The variation of the bond angle *hi*, which is related to the rehybridization of the carbon atoms from sp^2 to sp^3, also supports the previous statement since no important changes on *hi* are detected for $s < 1.0$. With regard to the bond angle between Os and the terminal oxygens (*ad*), it smoothly opens along the reaction path until a maximum of 121.3° is reached in **2c**. A similar trend is observed for the bond angle *ab*, the only exception being a slight decrease near the final ring ($4.1 < s < 4.5$). Notice that the olefinic carbons and the two oxygen atoms bonded to them remain coplanar along the entire reaction path, as indicated by the nearly constant value of the dihedral angle *egf* around 0°. The bond distances depicted by *a* and *d* also remain constant.

Base-Assisted Cycloaddition. The starting point for the study of the base-catalyzed dihydroxylation reaction is chosen here to be the adduct of stoichiometry $OsO_4 \cdot NH_3$, since kinetic studies suggest that only a single ligand molecule is involved in the rate-determining step.[40]

Figures 7 and 8 display the optimized molecular structures of the stationary points for the [2+2]- and

(40) Kolb, H. C.; Andersson, P. G.; Bennani, Y. L.; Crispino, G. A.; Jeong, K.-S.; Kwong, H.-L.; Sharpless, K. B. *J. Am. Chem. Soc.* **1994**, *116*, 8470.

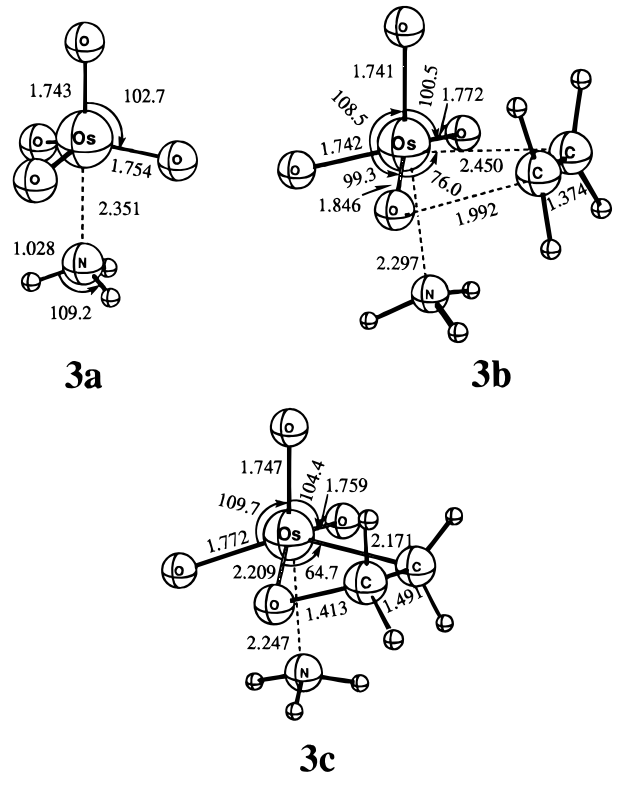

Figure 7. Optimized geometries for the stationary points along the base-assisted [2+2]-cycloaddition reaction path: **3a**, $OsO_4 \cdot NH_3$ complex; **3b**, transition state; **3c**, the osmaoxetane product. Bond lengths are in Å, and bond angles are in degrees.

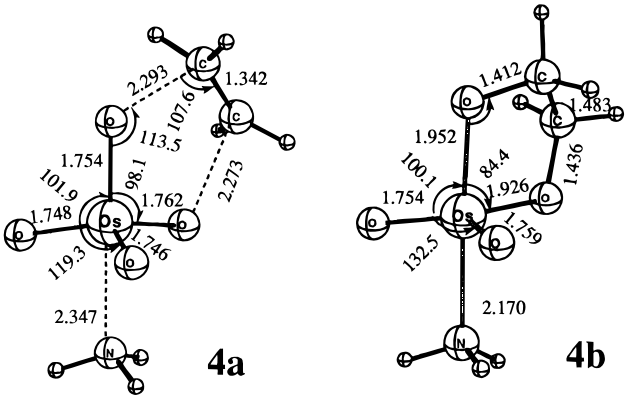

Figure 8. Optimized geometries for the stationary points along the base-assisted [2+3]-cycloaddition reaction path: **4a**, the transition state; **4b**, the five-membered ring product. Bond lengths are in Å, and bond angles are in degrees.

[2+3]-cycloaddition reaction paths, respectively. A comparison between these two figures and their corresponding analogs without NH_3 (Figures 1 and 4, respectively) reveals that the addition of a base does not affect significatively the way in which the reaction proceeds. However, a few points must be mentioned.

With regards to the [2+2]-cycloaddition reaction (Figure 1 vs Figure 7), the main difference is a slight delay of the base-free TS, **1b**, with respect to the base-assisted TS, **3b**, along the reaction path. For instance, the *R*(Os−C) distance in **3b** is 2.450 Å, whereas in **1b** it is closer to the final distance in the ring (2.379 Å). Also notice that the curvature of the energy profile around the TS **3b** is slightly less pronounced than around **1b**: the four lower frequencies of **3b** (−568, 31, 85, and 140 cm^{-1}) are numerically smaller than those of **1b** (see above). Another point of interest concerns the extent of interaction between olefin and the osmium complex. As can be seen from a comparison between **1c** and **3c**, a stronger interaction between the olefin and the catalyst is found in the final intermediate when the cycloaddition is base assisted. Thus, not only *R*(Os−C) and *R*(C−O) distances are shorter in **3c** than in **1c**, but also *R*(Os−O) and *R*(C−C) distances in the ammonia-free **1c** structure are not as long as in **3c**.

Regarding the [2+3]-cycloaddition reactions (Figure 4 vs Figure 8), similar conclusions can be drawn. Thus, here again the interaction between C_2H_4 and the osmium complex in the final intermediate has progressed further when ammonia is present (**4b**) than when the reaction is non-base assisted (**2c**). Notice that, since the four lower frequencies of the TS **4a** (−36, 67, 99, and 107 cm^{-1}) are even smaller than in the case of the TS **2b**, the reaction side of the base-assisted cycloaddition is expected to have an energy profile even flatter than in the case of the base-free cycloaddition. This partially explains why no adduct for the ammonia-assisted reaction has been found. Further, as already mentioned for the [2+2] cycloadditions, the base-free TS, **2b**, is also found to be remarkably later than the based-assisted TS, **4a**, along the reaction path. This is shown, for instance, by a shorter *R*(C−O) average distance in **2b** (2.04 Å) than in **4a** (2.28 Å).

At this point it is worthwhile mentioning that the calculations presented here can provide theoretical support to some structural assumptions made by Corey et al. in terms of molecular structures. Thus, conclusions drawn by these authors on a $^{12}C/^{13}C$ kinetic isotope effects investigation[15] were established by assuming that the postulated [2+2]-like transition state would resemble the metallaoxetane structure. As seen from Figures 1 and 7 in this paper, such assumptions can now be established as valid because of the similarity found between the structure of the productlike TS involved in the [2+2] mechanism and the structure of the final osmaoxetane (**1b** vs **1c** in Figure 1 and also **3b** vs **3c** in Figure 7).

On the other hand, the present results are in disagreement with an early remark by Sharpless and coworkers about the relative stabilities of the [2+2] and [2+3] intermediates, based on structural considerations.[10] According to these authors' hypothesis, a five-membered intermediate such as **2c** is not likely to be formed because of severe angle strain due to the long Os−O bonds.[41] By contrast, it was claimed that a four-membered intermediate such as **1c** should be substantially less strained since the long Os−C and Os−O bonds would have the effect of relieving the angle strain. It was also said that these objections to the [2+3] mechanism are only removed when prior coordination of a nucleophile to OsO_4 is invoked. From our investigation, it is in the four-membered intermediate (**1c** or **3c**) where there seems to be considerable strain, since one of the carbons is forced to get out of the plane, and the other three oxygen atoms suffer large distortion to make room for the first entering carbon atom. On the contrary, atoms manage to be accommodated well in the five-membered ring (**2c**), without losing so much the tetrahedral integrity of the OsO_4 fragment.

(41) (a) Conn, J. F.; Kim, J. J.; Suddath, F. L.; Blattmann, P.; Rich, A. *J. Am. Chem. Soc.* **1974**, *96*, 7152. (b) Collin, R.; Jones, J.; Griffith, W. P. *J. Chem. Soc., Dalton Trans.* **1974**, 1094.

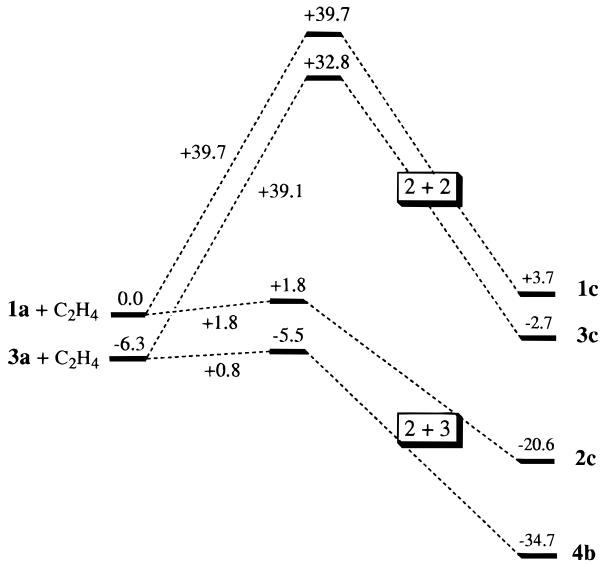

Figure 9. Schematic representation of the energetics involved in the [2+2]- and [2+3]-cycloaddition reactions, with and without ammonia. Energies are in kcal mol^{-1}.

From the energy point of view, a whole picture of the reaction barriers in osmium-catalyzed dihydroxylation of olefins can be obtained from Figure 9, which represents the energetics involved in the [2+2]- and [2+3]-cycloaddition reactions, with and without a ligand-base molecule (L = NH_3). The energy for the reactant species C_2H_4 + OsO_4 has been taken as zero. All energies are relative to this reference. Notice that the addition of NH_3 to OsO_4 stabilizes the system by 6.3 kcal mol^{-1}. Regarding the [2+2]-cycloaddition reactions, both the base-free and the base-assisted pathways involve large activation barriers (above 39 kcal mol^{-1}) and display similar energy profiles. Thus, the OsO_4-promoted dihydroxylation reaction is unlikely to proceed through a [2+2] mechanism (neither with nor without an added base). By contrast, the [2+3]-reaction paths have a very early TS and a much smaller activation barrier. In this case, the addition of a ligand base to the catalyst does substantially improve the feasibility of the reaction. Thus, as seen from Figure 9, when NH_3 is added the resulting activation barrier becomes less than half the barrier of the base-free cycloaddition (0.8 kcal mol^{-1} vs 1.8 kcal mol^{-1}). The assistance of a base in the reaction is even clearer in the stabilization of the final five-member intermediate, −20.6 kcal mol^{-1} without NH_3 (**2c**) vs −34.7 kcal mol^{-1} with NH_3 (**4b**).

Concluding Remarks

From the present investigation, there is enough evidence to rule out the [2+2] mechanism proposed by Sharpless and co-workers for the osmium-catalyzed dihydroxylation reaction of olefins. Our calculations indicate that such a [2+2] pathway has an activation barrier too high for the whole process to be feasible under the experimental reaction conditions (more than 39 kcal mol^{-1}).

On the other hand, the present results are not in contradiction with a two-step pathway involving a [2+3] transition state as suggested by Corey. In fact, such a mechanism seems to be very plausible from the calculations presented in this study, since only a low energy barrier of less than 2 kcal mol^{-1} is involved in the formation of the predicted five-membered species.

Although our results favor the mechanism proposed by Corey et al., we have been unable to optimize any weak olefin−Os(VIII) π−d complex, whose existence is postulated to precede the formation of the [2+3] TS. At this point several considerations must be taken into account. Since the binding energy between OsO_4 and NH_3 is theoretically predicted[18] to be about only 7−8 kcal mol^{-1}, a complex between OsO_4 and C_2H_4 (which is a weaker base than NH_3) should have an even smaller complexation energy. However, under experimental conditions, such a complex is not unlikely to exist because bulky substrates can easily bring the olefinic double bond close to the osmium-catalyst fragment in an appropriate geometry for further conversion to the TS. Our simple model, where the chain of the substrate has been substituted by a free C_2H_4 molecule, cannot reproduce these conditions. Therefore, despite our efforts to force the olefin to enter in a facial approach, we have not been able to report any π−d complex.

A comparison between the base-free and the base-assisted systems reveals that the addition of a ligand molecule is not crucial regarding the feasibility of one reaction path or another. The presence of a base enhances slightly the rate of formation of the five-membered ring while increasing its stability. On the whole, mechanistic conclusions drawn from the investigation of the base-free system are also suitable when the reaction is assisted with a base molecule.

Since further work is still required for a full understanding of these mechanisms, a more detailed investigation based on the results presented here will appear in a forthcoming paper. As a whole, the hypothesis suggested by Corey et al. seems to be more plausible to us and encourages us to continue studying the gradually sequence by which oxygen atoms are transfered to olefin in the metal-promoted dihydroxylation reaction of alkenes.

After the completion of this work two other groups[42] have independently reached the same conclusion as to the preference of the [2+3] addition over the [2+2] addition.

Acknowledgment. This work has been supported by the Natural Sciences and Engineering Research Council of Canada (NSERC), as well as by the donors of the Petroleum Research Fund, administered by the American Chemical Society (ACS-PRF No. 31205-AC3). We also acknowledge access to the computer facilities at the University of Calgary. One of us (M.T.) thanks the Direccio General de Recerca de la Generalitat de Catalunya for travel grants.

OM960783Q

(42) (a) Dapprich, S.; Ujaque, G.; Maseras, F.; Lledos, A.; Musaev, D. G.; Morokuma, K. *J. Am. Chem. Soc.* **1996**, *118*, 11660. (b) Pidun, U.; Boehme, C.; Frenking, G. *Angew. Chem.*, in press.